THE ASTROPHYSICAL JOURNAL, 374:319–329, 1991 June 10

BROAD-BAND LINEAR POLARIZATION IN COOL STARS. I. MODELS AND SPATIAL EFFECTS FOR MAGNETIC AND SCATTERING REGIONS

JUHANI HUOVELIN
Observatory and Astrophysics Laboratory, University of Helsinki, Tähtitorninmäki, SF-00130, Helsinki, Finland

AND

STEVEN H. SAAR
Harvard-Smithsonian Center for Astrophysics, MS 58, 60 Garden Street, Cambridge, MA 02138
Received 1990 May 25; accepted 1990 October 23

ABSTRACT

We have developed models of broad-band linear polarization (BLP) arising from magnetic regions on cool stars. The models include an improved treatment of spatial effects in which the BLP is explicitly integrated over the stellar surface. We find that for magnetic region filling factors, f, larger than $\approx 1\%$ of a hemisphere, direct disk-integration yields results which are often significantly different from a simple linear scaling of BLP with region area, especially for regions near the limb. In particular, the amplitude of the BLP reaches a maximum for $f \approx 24\%$, which is a consequence of cancellation of the polarization signal within the region itself. The line-of-sight angle at which the region exhibits maximum polarization increases with region size.

We study the effects of bipolar pairs of regions, and single regions with small-scale bipolarity. The most important effect of bipolarity is the reduction in the influence of Faraday rotation on the integrated polarization. Spatial effects become more important as the size of the bipolar spot pair is increased.

We construct similar models for Rayleigh and Thomson scattering regions in order to compare the signatures of BLP from these sources. Like magnetic BLP, scattering-induced BLP shows a maximum in polarization amplitude (at $f \approx 18\%$), but the line-of-sight angle of the maximum first decreases (for $f \leq 10\%$) and then increases with increasing region size. We also present approximate formulas for the scaling of magnetically induced and scattering-induced polarization as a function of f. We discuss the importance of the differences found in the rotational phase dependence for discerning the source of the polarization. Use of the phase dependence requires detailed comparisons of polarization observed at several rotational phases, with the success of application depending on the specific geometry of the polarizing regions. The general applicability of the models depends on the accuracy in determining the instrumental and interstellar polarization (in modeling of polarization degree P) and/or the orientation of the stellar rotation axis on the plane of the sky (in modeling of Stokes parameters P_Q and P_U).

Subject headings: polarization — stars: late-type — stars: magnetic

1. INTRODUCTION

Broad-band linear polarization (BLP) has been observed in many cool stars over the past decade (e.g., Piirola 1977; Barbour & Kemp 1981; Tinbergen 1982; Hayes 1984; Huovelin et al. 1985, 1989). Although in red giants it may be partly the result of Thomson or Rayleigh scattering from the photosphere and chromosphere, or scattering from dust grains (e.g., Doherty 1986; Huovelin et al. 1987; McCall & Hough 1980), BLP in most late-type dwarfs probably arises from an inhomogeneous distribution of magnetic regions (Tinbergen & Zwaan 1981). The σ and π components of optically thick lines formed in areas with magnetic fields will have differing saturation characteristics—the so-called magnetic intensification (MI) effect. Because of this effect, a net linear polarization results, which, integrated over all lines in a given passband, produces the observed BLP (e.g., Leroy 1962; Kemp & Wolstencroft 1974; Mullan & Bell 1976).

Time series of BLP measurements have considerable potential in unraveling the spatial configuration of magnetic regions on stellar surfaces due to the strong geometric dependence of the polarization amplitude and direction. In particular, multiple observations of BLP can help to determine the stellar inclination angle (e.g., Landi Degl'Innocenti et al. 1981), and rough locations of the dominant active regions (Landi Degl'Innocenti 1982, hereafter L82). With these possibilities in mind, models of the expected behavior of linear polarization in cool stars have been introduced (Finn & Kemp 1974; Calamai, Landi Degl'Innocenti, & Landi Degl'Innocenti 1975; L82; Landi Degl'Innocenti & Calamai 1982; Calamai & Landi Degl'Innocenti 1983, hereafter CL). These models are incomplete in their treatment of geometric effects, however. The effects of finite sizes of magnetic regions are treated in a very approximate fashion, which leads to errors in the derived stellar BLP.

We have developed an improved model of stellar BLP which includes a more complete treatment of the spatial effects. We report the results for several distributions and sizes of magnetic regions on stellar surfaces as a function of rotational phase, and explore the effects of bipolar regions. Since Rayleigh and Thomson scattering can also be sources of linear polarization (e.g., Finn & Jefferies 1974), we construct a similar model to compare scattering-induced with MI–induced BLP. We also discuss methods of distinguishing between magnetic fields and scattering as sources of BLP.

2. THE MAGNETIC POLARIZATION MODEL

2.1. *Development of the Model*

In L82 and subsequent papers, the expected BLP from pointlike magnetic sources on a stellar surface is computed as a function of location on the star and the orientation of the star to the observer. A linear scaling (filling factor) is then applied to determine the expected BLP from a magnetic region of finite size. This method ignores the self-canceling effects which arise from the *vector sum* of the BLP from regions larger than a point. The linear scaling systematically overestimates BLP from active areas by progressively larger amounts as the filling factor, f, of the region increases. Indeed, at some point, the total BLP will *decrease*, even as f increases. As an extreme example, stars devoid of active regions and stars completely covered with a uniform radial magnetic field will both give rise to *zero* net BLP (e.g., Huovelin, Saar, & Tuominen 1988; Landolfi, Landi Degl'Innocenti, & Landi Degl'Innocenti 1989).

The self-canceling effect will be negligible for small (solar-like) active regions which cover only a few thousandths of the stellar disk. Considerable evidence points to much larger active regions on other stars, however. In particular, RS CVn systems, BY Dra variables, T Tauri, W UMa, and FK Comae stars and some active dwarfs all show photometric modulation due to starspots. In many cases, the filling factors of dark spots alone can approach 20%–30% of the stellar surface (e.g., Poe & Eaton 1985; Rodonò et al. 1986), and by analogy with the Sun, spot umbrae will probably comprise only a fraction of the total magnetic region area. Brighter areas, such as plages, magnetic network, and penumbrae can be expected to dominate the filling factor of active regions (e.g., Cayrel et al. 1983). Thus, at least for the more active stars, we anticipate that the linear scaling of BLP with the magnetic region filling factor will break down.

To correct this shortcoming, we have constructed an improved model for stellar BLP by introducing explicit disk integration to the L82 form. An outline of the model and results is given in Huovelin & Saar (1990). We begin by assuming that the BLP from a given element on the stellar surface can be approximated by using an "average" line profile computed for the ψ (the angle between the magnetic field and the line of sight) and ϕ (the azimuthal angle of the field, with its zero point at the projection of the stellar rotation axis on the sky) of the element (see Calamai et al. 1975). The line models are based on a Milne-Eddington atmosphere in LTE with a linear source function, including magneto-optical effects (i.e., Faraday rotation). The BLP values are calculated using the mean values for the line-to-continuum opacity ratio (η_0), Doppler witdh ($\Delta\lambda_D$), magnetic sensitivity (Landé $g_{\rm eff}$), magnetic field strength (B), and the Voigt parameter (a). The angle that the magnetic field makes with the normal to the stellar surface, θ, is assumed to be 0° everywhere in the photosphere (a reasonable approximation in the Sun; e.g., L82), and so $\theta = \psi$. The net BLP from the surface element in the computed line is calculated by integrating $P_Q = Q/I$ and $P_U = U/I$, the normalized Stokes parameters, over all wavelengths. The result is scaled with the average fractional line blanketing in the wavelength region (ξ) to obtain the expected BLP for a given bandpass, yielding

$$P_Q = C\,\frac{3}{2}\,\frac{\xi}{1-\xi}\cos\psi\,\Pi(\psi, v_B)\cos\{2[\phi + \Phi(\psi, v_B)]\}\,, \quad (1)$$

and

$$P_U = C\,\frac{3}{2}\,\frac{\xi}{1-\xi}\cos\psi\,\Pi(\psi, v_B)\sin\{2[\phi + \Phi(\psi, v_B)]\}\,, \quad (2)$$

where $v_B = \Delta\lambda_B/\Delta\lambda_D$ and $\Delta\lambda_B = 4.67 \times 10^{-13}\lambda^2(\text{Å})g_{\rm eff}\,B$. The Π and Φ functions are defined as in Calamai et al. (1975), as modified to include Voigt parameters by CL. We obtain the Π and Φ functions for our chosen average parameters by spline interpolation directly from the tables of Landi Degl'Innocenti & Calamai (1982) and CL. Thus far, our formulation is identical to that of L82, with the exception of the correction factor C. The correction term $C(\leq 1)$ includes the reduction of polarization due to molecules (which show little polarization) and line blending. In this paper, we are primarily interested in dependence of BLP on active region geometry and in *relative* changes in polarization produced by varying magnetic area coverage. Since C affects only the *absolute* level of the polarization and not the angular (i.e., geometric) dependence, its precise value is not critical for our models, as we assume $C = 1$. This approximation is valid if the portion of the spectrum modeled is not heavily blended and contains few molecular lines. As pointed out by Leroy (1989, 1990), neglecting the effects of blends and molecules may lead to considerable overestimates of the linear polarization, especially in the crowded ultraviolet spectra of solar-like stars. The solar U-band polarization, for example, is overestimated by a factor of 2 if blends are not considered. The above effects will be discussed in detail by Saar & Huovelin (1990a, hereafter Paper II).

At this point, however, instead of scaling the point source BLP with a linear area coverage factor $A\cos\psi/\pi R_*^2$ (L82), we perform disk integration of the BLP over the stellar surface. For our model star, we use an equal area grid with 30 radial and 120 azimuthal steps; experiments with finer grids altered the results by less than a few percent for areas larger than $\sim 1\%$ of a stellar hemisphere. For smaller areas we use denser grids to reduce artificial, stepwise changes in the derived BLP. The (equal) fractional projected area of the surface elements implicitly accounts for the projection ($\cos\psi$) effect on the net BLP, and cancellation of the polarization within individual elements is negligible. The actual integration of the net BLP over the spatial extent of the magnetic region(s) allows a considerably more realistic treatment of the cancellation effects.

In the following we use the term "spot" to designate *any* magnetic region; we do not mean to imply that the areas under consideration have to be cool like solar umbrae. Regions considerably cooler than the average surrounding photosphere are less important (and probably negligible) in the disk-integrated linear polarization, due to their minimal contribution to the integrated *light*. Indeed, the umbral contribution is weakest in the U band, precisely where the high density of lines suggests that BLP should be large.

2.1. *Tests and Comparison with Unipolar Regions*

The following parameters were assumed throughout: $\eta_0 = 10$; $\lambda = 6000$ Å; $\xi = 0.10$; $v_B = 1.2$; $g_{\rm eff} = 1.5$; $a = 0.1$. The effects of different values of these parameters have been investigated by CL and others. Tests of the derived BLP in the limiting cases of zero and complete coverage by magnetic fields gave the appropriate value (i.e., zero) for the BLP to within one part in 10^6 (limit of the numerical accuracy).

In his paper (L82), Landi Degl'Innocenti studies the variation of P_Q and P_U with rotation for various spot latitudes and stellar inclination angles. We reproduced the eight linearly scaled models presented in L82 (Figs. 2 and 3 in L82) with $A/\pi R_*^2 = 0.1$, corresponding to a unipolar (positive polarity) region with a filling factor $f = 5\%$ of a hemisphere (i.e., $f = A/2\pi R_*^2 = 0.05$; hereafter all percentage spot areas refer to this parameter, unless otherwise stated), and we compared them with our new disk-integrated models, obtained with identical

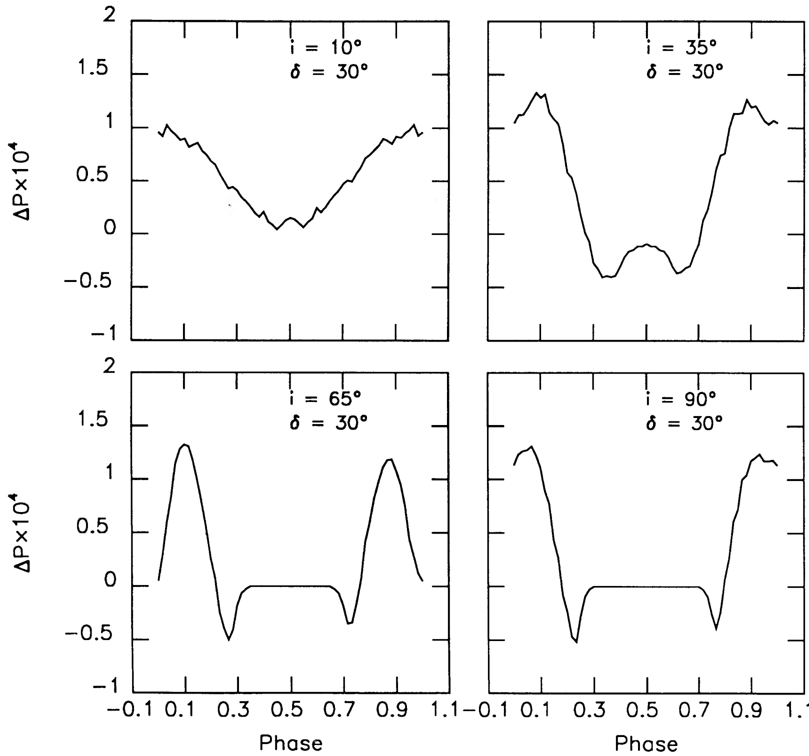

FIG. 1.—The difference $\Delta P(\equiv P_{L82} - P_{DISK\text{-}INT})$ between the disk-integrated models ($P_{DISK\text{-}INT}$) and the linearly scaled models (P_{L82}) for different stellar inclinations (i) (see also Fig. 2 in L82).

input parameters. The Stokes parameters in both sets of models were multiplied by 10^4 to obtain the scaling used in L82. The models were calculated in 61 equally spaced phases from 0 to 1.

The overall shapes of the Stokes P_Q versus P_U loci were close to those in Figures 2 and 3 of L82, which were calculated using linear scaling of BLP with spot area, but the disk integration yielded consistently smaller amplitudes of the variations (i.e., the sizes of the loci were smaller). The differences $\Delta P(\equiv P_{L82} - P_{DISK\text{-}INT})$, where $P \equiv (P_Q^2 + P_U^2)^{0.5}$ is the polarization degree, are plotted in Figures 1 and 2. The maxima of the relative overestimates due to linear scaling in these models ($f = 5\%$) are approximately 20%–30% of the total rotational polarization variations.

Qualitatively, the results shown in Figures 1 and 2 are approximately valid for a spot with $1\% \leq f \leq 50\%$, with the only significant difference being the *relative* amount of over- or underestimate, which increases with spot size. This behavior is clearly exhibited in Figure 3, which shows models (with $i = 90°$) of P as a function of spot size and the angle on the stellar surface between the disk center and spot center (line-of-sight angle). The line-of-sight angle at which the overestimates of polarization due to linear scaling turn to underestimates changes only slightly with spot size, from about 70° for a $f = 2\%$ spot to about 76° for $f = 50\%$. The underestimated P_{L82} values are due to the simple cosine law used for the projection effect in the linear scaling model. As an extreme example, the cosine approximation yields zero projected area for all spots which are more than half behind the limb, if further modifications for partial visibility are not made. Overestimates of P_{L82} in the central area of the disk, on the other hand, result from the neglect of self-cancellation of polarization *within* the spot, which becomes more and more important with increasing spot size. This difficulty can only be properly addressed by using a disk integration method with a sufficiently dense grid on the stellar surface. Our tests showed that linear scaling and disk integration yield essentially identical results (relative difference $< 5\%$) with unipolar spots smaller than 1% of a hemisphere. However, the maximum overestimate due to linear scaling increases rapidly with spot size and is already 17.5% for an $f = 4\%$ spot and about 100% for $f = 16\%$ (see Figs. 3 and 4).

Figure 3 also shows how the line-of-sight angle of the maximum polarization increases with spot size, an effect which can only be seen by employing disk integration, since linear scaling yields the maximum polarization at 45° from disk center, independent of the spot size (in Huovelin et al. 1988, the limb darkening coefficient was incorrectly mentioned to affect the line-of-sight angle of maximum polarization). A secondary maximum in the polarization also appears at 30° in the disk integration model for $f = 50\%$ spots (Fig. 3). Its appearance is actually a consequence of a minor decrease in polarization at larger angles, caused by the increasing fraction of the spot behind the stellar limb. The polarization increases again when substantial numbers of surface elements which used to cancel the BLP of other elements in the spot are placed behind the limb. The secondary maximum is resolved from the primary maximum for spots with $f > 40\%$.

Fundamental to all the above effects caused by the self-cancellation of spot polarization, however, is the nonlinear increase of the maximum polarization with spot size (Fig. 4). The maximum P reaches an upper limit for $f \approx 24\%$ and there-

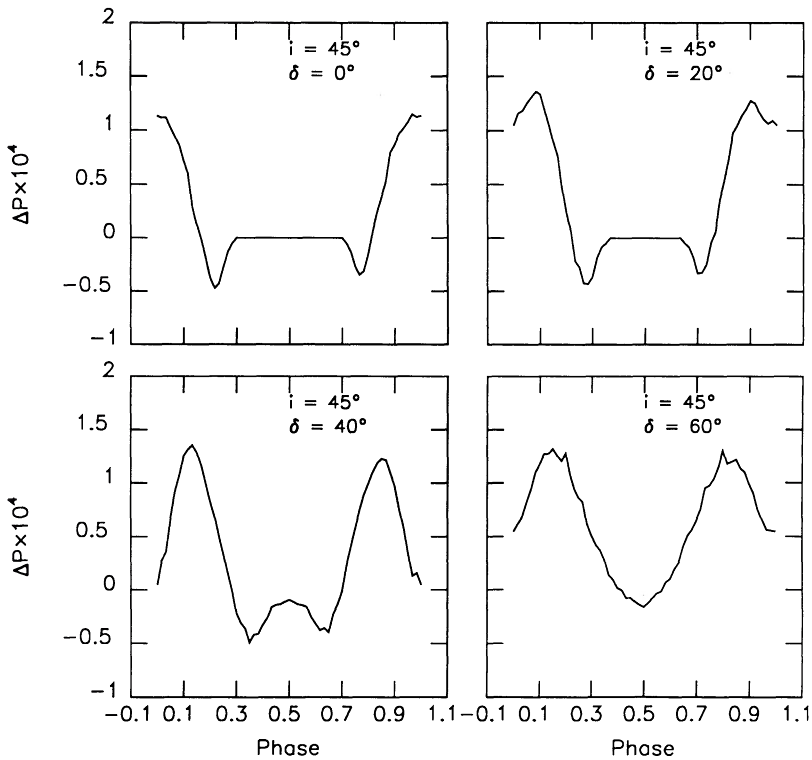

FIG. 2.—The difference ΔP between the disk-integrated models and the linearly scaled models for different spot latitudes (δ) (see also Fig. 3 in L82)

after decreases with increasing spot size. A spot can actually contain surface elements which completely cancel the BLP of other elements (two identical elements equally distant from the disk center but with a 90° difference in azimuth will completely cancel each other, for example). By fitting a polynomial to the $P_{max}(f)$ curve in Figure 4, we obtain the following approximate formula,

$$\frac{P_{max}(f)}{P_{max}(f = 1\%)} \approx -2.128 \times 10^{-2} + 1.076f - 4.812 \times 10^{-2}f^2 + 9.058 \times 10^{-4}f^3 - 6.26 \times 10^{-6}f^4 , \quad (3)$$

where f is given in percent. The above scaling is valid for $f \leq 50\%$, and it should be applied separately for each individual region. For example, two identical regions equidistant from the stellar disk center and separated by $\pm 180°$ in ϕ would yield exactly twice as large P as one region, since linear polarization is invariant under 180° rotations on the plane of the sky. More generally, one can roughly derive the maximum total polarization with several regions by first scaling the Stokes parameters P_Q and P_U for each spot, and then performing a vector sum of the contributions of all spots. Assuming that the stellar surface contains one major magnetic region, expression (3) can be used in approximate determinations of lower limits for filling factors, as it gives the maximum of polarization during rotation. A demonstration of such a filling factor determination is presented in Paper II.

In L82 it is mentioned that the shapes of the P_Q, P_U diagrams are not affected significantly by changes in line strength (η_0) and magnetic field (v_B) values. We found this to be valid in only a limited sense. The angles of the maximum polarization and equation (3) are approximately valid over a wide parameter range (we found $\leq 5\%$ relative difference from equation [3] with the following ranges: $\eta_0 = 10$–100, $B = 500$–3000 G, $a = 0.05$–0.2), and the qualitative effects of spot size remain unaffected by changes in η_0, B and damping a. This implies that Figure 3 shows the general behavior of MI-induced polarization (within the limits set by the simplifying initial assumptions of the model). On the other hand, while it is true that the overall *shapes* of the diagrams resemble each other for a wide range of η_0 and B, the scaling factor *between* diagrams is a

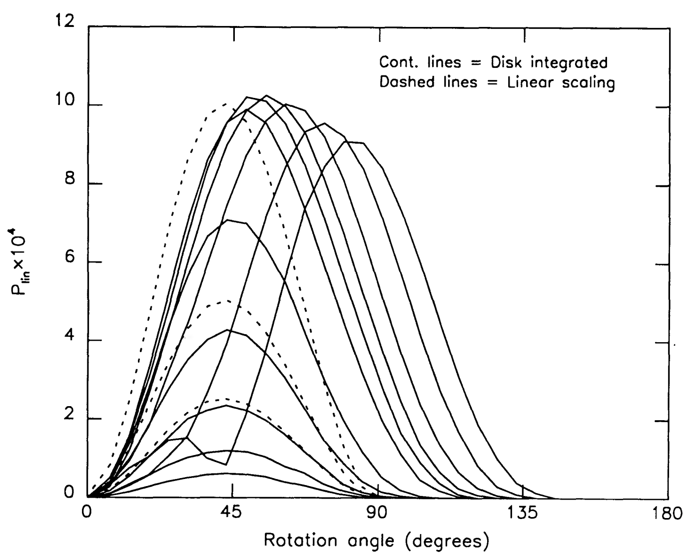

FIG. 3.—The degree of linear polarization vs. the line-of-sight angle (i.e., rotation angle) for spots with filling factors $f = 0.5$, 1, 2, 4, 8, 16, 20, 24, 30, 40, and 50%. The angle of the maximum polarization increases with spot size. The linear scaling result is shown (*dashed*) for spot with $f = 2$, 4, and 8%.

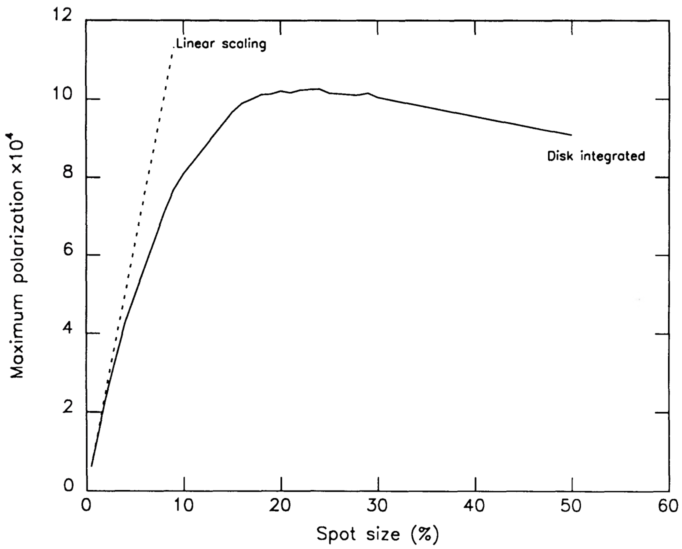

FIG. 4.—Variation of maximum polarization with spot size. Disk-integration models exhibit the largest polarization for spots covering 24% of the hemisphere; the differences with linear scaling (*dashed line*, L82) increase rapidly with spot size.

function of ψ (or rotational phase φ). As an example, we calculated the L82 model with $i = 45°$ and $\delta = 60°$ for $\eta_0 = 10$ and 100. The ratio $P(\varphi)_{100}/P(\varphi)_{10}$ varied from 0.43 to 0.56 with $B = 500$ G and from 0.43 to 0.70 with $B = 3000$ G. The effect of large changes in B on $P(\varphi)$ ratios is even stronger. $P(\varphi)_{3000\,\mathrm{G}}/P(\varphi)_{500\,\mathrm{G}}$ varied from 7.9 to 17.5 ($\eta_0 = 10$), and from 9.8 to 17.1 ($\eta_0 = 100$). The relative scaling of polarization [i.e., the ratios $P(\varphi, f_1)/P(\varphi, f_2)$ in Fig. 3] is therefore exactly valid only with the given parameters. The reason for the variations in the $P(\varphi)$ ratios arises from the changing optical thickness in the linear polarized Zeeman components as a function of φ. As one alters η_0 or B, the saturation and the degree of blending between the π and σ components change, thus changing the ratio at a given φ.

2.2. *Bipolar Spot Pairs and Regions with Mixed Polarities*

The magnetic areas on the Sun, and probably on most solar-like stars, have bipolar structure, with close pairs of regions having opposite magnetic field polarities (e.g., Borra, Edwards, & Mayor 1984). As shown in L82, a bipolar spot pair will produce polarization variations with reduced effect of the Faraday rotation (i.e., loops in the P_Q, P_U plane are less asymmetric with respect to the P_U-axis). In the limiting case when the spots are like point sources very close to each other, the Faraday rotation is completely canceled, and the loop shapes above and below the P_U-axis are identical. In terms of rotational phase, φ ($\varphi = 0$ when the bipolar spot pair passes the central meridian of the stellar surface), $P_U(\varphi) = -P_U(-\varphi)$ and $P_Q(\varphi) = P_Q(-\varphi)$ (see L82). In physically realistic cases, however, surface elements with opposite polarities cannot overlap, and the regions have finite sizes. Geometric effects will influence the resulting polarimetric variations, especially if the two regions of opposite polarities are large and therefore widely separated.

Since it is not yet clear whether the unipolar fractions of the magnetic areas can be considerably larger in some stars relative to the Sun, we modeled two extreme cases. In model (1) we have a "checkerboard" structure of polarities inside a $f = 5\%$ circular region, with surface elements of positive and negative polarities evenly mixed throughout the spot. In model (2), the magnetic area is split into a pair of circular spots of equal size ($f = 2.5\%$) and opposite polarity, separated by 26° in stellar longitude (the minimum separation allowed without overlap).

Figures 5 and 6 show the results with the above two models. The differences between the models depend strongly on the geometry (i.e., δ and i), and are significant in all cases shown. It is obvious that the difference will increase as the sizes of the opposite polarity regions increase, while case (2) approaches case (1) as the sizes and separation distance of the bipolar spot pair are decreased, keeping f in the two cases equal. In practice, the shapes of the loops with small spots are nearly identical with those produced by two (hypothetical) completely overlapping, opposite polarity regions. Thus, remembering the limitations of the linear scaling approximation (see Fig. 4), the simpler theory presented in L82 can be used in modeling the polarizations of stars with small ($f < 1\%$), solar-like magnetic regions.

3. COMPARISON WITH RAYLEIGH AND THOMSON SCATTERING

Rayleigh scattering also produces BLP, which can confuse the interpretation of polarization measurements. Possible sources of Rayleigh scattering in late-type stars include extended, inhomogeneous envelopes, chromospheres and photospheric spots. Stars with chromospheres may also have enough free electrons to cause linear polarization via Thomson scattering, similar to the envelopes of early-type stars (e.g., Serkowski 1970, Brown and McLean 1977, and references therein), and binary stars (e.g., Shakhovskoi 1965; Piirola 1980). The spatial distribution of the scattering medium may, however, be somewhat different in cool stars, and the models for special cases of early-type stars and binaries may not directly apply. It is therefore important to derive models suitable for the atmospheres of cool stars and to investigate ways to distinguish between scattering and MI as sources of BLP, since neither one can be rejected as a source of BLP using simple arguments.

3.1. *Comparison of Phase Dependence and Scales*

We model the BLP due to single (either Rayleigh or Thomson) scattering starting from the theory for particles with isotropic polarizability, presented in van de Hulst (1957). The scattering medium is assumed optically thin, and the incident light is assumed unpolarized. The relevant Stokes parameters (in the local coordinate system) for the intensity I'_0 scattered from an atmospheric element (of volume dV) toward the observer will be

$$dI = dI_0(1 + \cos^2 \psi')dV , \quad (4)$$

$$dQ = dI_0 \sin^2 \psi' \cos\left[2\left(\varphi' + \frac{\pi}{2}\right)\right]dV , \quad (5)$$

$$dU = dI_0 \sin^2 \psi' \sin\left[2\left(\varphi' + \frac{\pi}{2}\right)\right]dV , \quad (6)$$

where

$$dI_0 = I'_0(\theta, \phi')\,\frac{3n(r, \psi, \phi)}{16\pi r^2}\,\sigma_s(r, \psi, \phi)d\omega . \quad (7)$$

Here $n(r, \psi, \phi)$ is the number of particles per unit volume, σ_s is the scattering cross section per scattering particle, and $dV = r^2\,dr \sin\psi\,d\psi\,d\phi$. The angles ψ and ϕ are defined as in the MI model, and ψ' is the scattering angle of the incident light, coming from the direction of the solid angle $d\omega$

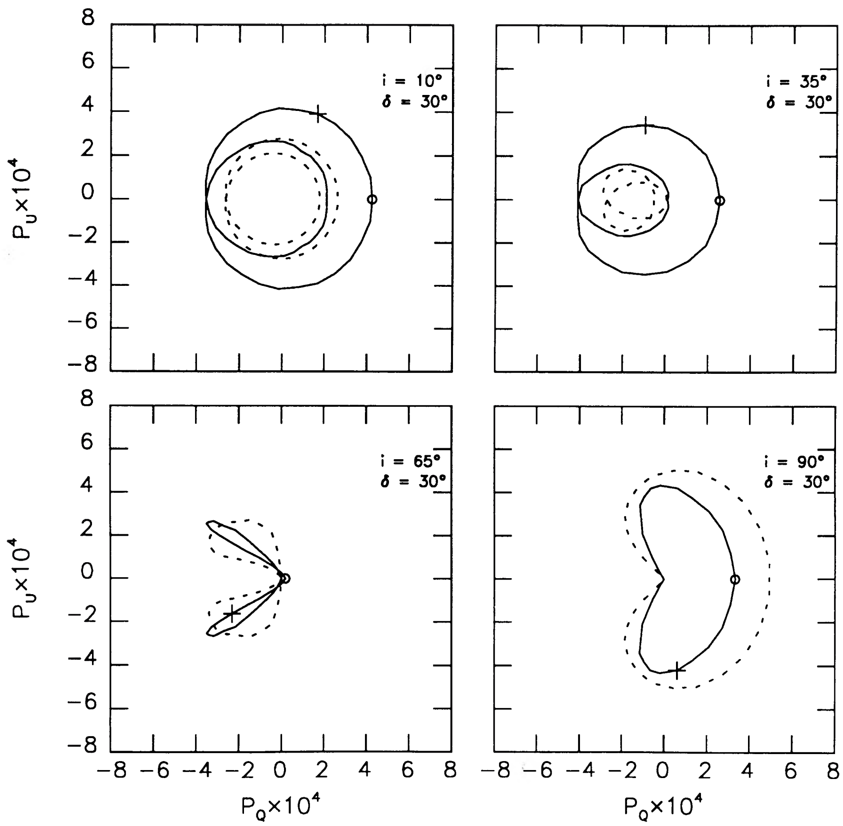

FIG. 5.—Models with bipolar magnetic field structures and different stellar inclinations. The solid line corresponds to one spot of size $f = 5\%$ with small-scale bipolar elements ("checkerboard"), and dashed line is the result for a bipolar pair with $f = 2 \times 2.5\%$. Zero phase is indicated with a circle, and phase 0.1 with a plus sign.

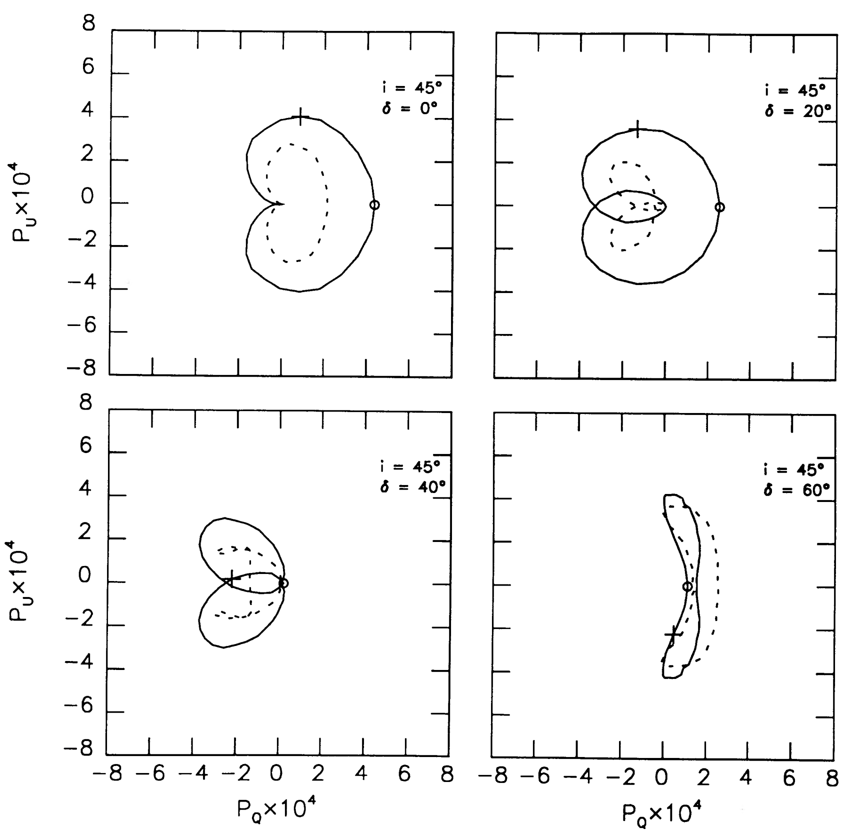

FIG. 6.—As in Fig. 5, but for spots with different latitudes

($=\sin\theta\,d\theta\,d\phi'$). The local polarization angle φ' is measured counterclockwise from the radius vector of the stellar disk. The local coordinates are defined so that θ is the angle from the surface normal at point (ψ, ϕ), and ϕ' is the local azimuth angle on the surface, measured counterclockwise from the direction to the disk center defined by the observers' frame.

Thus far the formulation has been quite general, and we have not made any assumptions about I'_0. Assuming spatially uniform intensity on a plane surface under the scattering layer with the intensity distribution similar to the solar surface with limb darkening, the intensity distribution incident on the element of the scattering layer will be $I'_0(\theta, \phi')d\omega = I_0(\psi, \phi)(1-\epsilon+\epsilon\cos\theta)d\omega$, where $I_0(\psi, \phi)$ is the surface brightness. With the plane approximation, we implicitly assumed that the scattering layer is geometrically thin (thickness $\ll$ stellar radius) and close to the stellar surface. The limitations are reasonable in the atmospheres of single cool stars, with chromospheres not much different from that of the Sun. The approximation is similar to that of Schwarz and Clarke (1984), with differences in the incident radiation field (Schwarz and Clarke considered only the radial intensity) and in the distribution of the scattering layer (Schwarz and Clarke assumed a uniform layer with inhomogeneous incident intensity). Applications in cases with extended clouds very far from the stellar surface can be found in Brown & McLean (1977) and Brown, McLean & Emslie (1978), while intermediate cases are discussed in, for example, Shulov (1967), and applied by Piirola (1980).

Now we integrate the incoming intensity distribution over the solid angle to find the functional dependence of Stokes parameters on ψ. From the symmetry of the intensity distribution, i.e., $I'_0(\theta, \phi') = I'_0(\theta, 2\pi - \phi')$, we notice immediately that the scattering plane will be that determined by the local radius vector and the line of sight. By defining the projection of the radius vector on the sky as the local positive Q-axis, we find that the local U will be canceled out in the integration. Deviations from the above symmetry will generally complicate the situation, which is demonstrated by detailed calculations of sunspot polarization by Finn & Jefferies (1974).

In our local coordinate system, the scattering angle (ψ') and the local position angle of linear polarization (φ') can be derived with the scalar and vector products of the incident direction unit vector, $\bar{a} = (\sin\theta\cos\phi', \sin\theta\sin\phi', \cos\theta)$, and the unit vectors $\bar{e}_x = (\sin\psi, 0, \cos\psi)$, $\bar{e}_y = (0, 1, 0)$, and $\bar{e}_z = (-\cos\psi, 0, \sin\psi)$ of the right-handed rectangular coordinate system, where e_x is directed toward the observer, and $\bar{e}_y$ is directed tangentially to the stellar surface. The cosine of scattering angle is $\cos\psi' = \bar{a}\cdot\bar{e}_x$, and the direction of the polarization vector on the plane of the sky is defined by $\cos\varphi' = (\bar{e}_x \times \bar{a})\cdot\bar{e}_y/|\bar{e}_x \times \bar{a}|$ (positive Q-axis coincides with $\bar{e}_z$). Substituting, we find that $\sin^2\psi' = 1 - (\bar{a}\cdot\bar{e}_x)^2 = |\bar{e}_x\times\bar{a}|^2$, which leads to $\sin^2\psi'\cos 2\varphi' = 2[(\bar{e}_x\times\bar{a})\cdot\bar{e}_y]^2 - |\bar{e}_x\times\bar{a}|^2$. By integration over the solid angle, we obtain the following formulae for the nonzero Stokes parameters in the local frame:

$$\begin{aligned}\int_\omega dI &= \int_0^{2\pi} d\phi' \int_0^{\pi/2} d\theta\,\sin\theta\,dI_0(1+\cos^2\psi')dV \\ &= I_0\,\frac{3n}{16\pi r^2}\,\sigma_s \int_0^{2\pi}\int_0^{\pi/2} \sin\theta(1-\epsilon+\epsilon\cos\theta) \\ &\quad\times[1+(\sin\theta\cos\phi'\sin\psi+\cos\theta\cos\psi)^2]d\phi'\,d\theta\,dV \\ &= I_0\,\frac{n}{2r^2}\,\sigma_s\left(1-\frac{17\epsilon}{32}+\frac{3\epsilon}{32}\cos^2\psi\right)dV\,, \end{aligned}\tag{8}$$

and

$$\begin{aligned}\int_\omega dQ &= \int_0^{2\pi} d\phi' \int_0^{\pi/2} d\theta\,\sin\theta\,dI_0\,\sin^2\psi'\cos\left[2\left(\varphi'+\frac{\pi}{2}\right)\right]dV \\ &= -\frac{3n}{16\pi r^2}\,\sigma_s \int_0^{2\pi}\int_0^{\pi/2} I_0\sin\theta(1-\epsilon+\epsilon\cos\theta) \\ &\quad\times[(\sin\psi\cos\theta-\sin\theta\cos\phi'\cos\psi)^2 \\ &\quad-(\sin\theta\sin\phi')^2]d\phi'\,d\theta\,dV \\ &= -I_0\,\frac{3n\epsilon\sigma_s}{64r^2}\sin^2\psi\,dV\,. \end{aligned}\tag{9}$$

Note that the contribution of the constant term $(1-\epsilon)$ in the intensity distribution is zero in integral in equation (9). By integrating equations (8) and (9) over the depth of the scattering layer (R) we obtain approximate formulas for the Stokes parameters as a function of the scattering optical depth $\tau_s = \bar{n}(\psi, \phi)\sigma_s R$, where $\bar{n}(\psi, \phi)$ is the mean number density of scattering particles in the stellar atmosphere. We use τ_s as the depth parameter in order to obtain more general expressions for the Stokes parameters which are valid for both molecules and electrons. The total scattering optical depth can be estimated separately, including the total scattering coefficient and the mean number density of all molecules and electrons. Finally, integration over the visible stellar surface (i.e., over ψ and ϕ) yields the total linear polarization Stokes parameters in the frame where the positive Q-axis lies along the projection of the stellar rotation axis on the sky. The total intensity of the stellar light is the sum of the direct unpolarized light and the scattered light:

$$\begin{aligned} I &\approx \int I_0(\psi, \phi)\cos\psi(1-\epsilon+\epsilon\cos\psi)dA \\ &\quad+\int I_0(\psi, \phi)\frac{\tau_s}{2}\left(1-\frac{17\epsilon}{32}+\frac{3\epsilon}{32}\cos^2\psi\right)dA\,, \end{aligned}\tag{10}$$

where $dA = \sin\psi\,d\psi\,d\phi$ and ϵ is the limb-darkening coefficient ($\epsilon = 0.6$ assumed here). The *normalized* Stokes parameters will thus be

$$P_Q \approx \frac{\int I_0(\psi, \phi)(3/64)\epsilon\tau_s\sin^2\psi\cos\{2[\phi+(\pi/2)]\}dA}{I}\,, \tag{11}$$

$$P_U \approx \frac{\int I_0(\psi, \phi)(3/64)\epsilon\tau_s\sin^2\psi\sin\{2[\phi+(\pi/2)]\}dA}{I}\,. \tag{12}$$

Note that these formulae apply to scattering either from atoms and molecules or free electrons, with $\sigma_s = 0.67\times10^{-24}(\lambda_0/\lambda)^4$ cm^2 for the former, where λ_0 is the characteristic "resonance wavelength" of the scatterer, and $\sigma_s = 0.67\times10^{-24}$ cm^2 for free electrons (e.g., Aller 1953). Another, equally valid expression for the Rayleigh scattering cross section for atoms and molecules, $\sigma_s = \alpha^2 128\pi^5/3\lambda^4$, is given in Allen (1955). Here α is the polarizability which is in simple cases (nearly spherical molecules) proportional to the effective "volume" of the scatterer, as seen by the scattered light beam.

The form of variation with $\mu = \cos\theta$ is similar to that of Collins (1988), i.e., $P = c1\times(1-\mu^2)/(1+c2\times\mu+c3\times\mu^2)$, where $c1$, $c2$, and $c3$ are constants determined by limb darkening and optical depth. The differences in the constants are basically due to our optically thin (single-scattering) approximation (Collins used detailed radiative transfer calculations of scattering in a magnetized atmosphere). We have also not made any assumptions as to the direct effects of magnetic field on the scattering. Our approximation would, for example, yield the same polarization at limb as the specific case of Collins ($c1 = 0.1153$), if we used $\epsilon = 0.74$, which is only slightly different from the solar limb darkening constant in the visual continuum ($\epsilon \approx 0.6$). This comparison demonstrates that our simple treatment of radiative transfer is sufficient for approximating the center-to-limb variations as well as the actual scale of scattering-induced linear polarization. We can obtain a reasonable upper limit for the polarization by taking $\tau_s = 0.1$, since double or multiple scattering will dominate for optical depths larger than the above value (van de Hulst 1957), and the polarization will be reduced due to the partial canceling of polarization in multiply scattered light (e.g., Shakhovskoi 1965).

To facilitate comparisons with the MI case, we computed eight scattering models with enhanced densities of scattering material at the same size and locations of the magnetic spots in the MI models. Note, that our models differ from those of Schwarz & Clarke (1984) and Doherty (1986) in that they assume anomalies in the optical depth (τ_s) instead of those in the brightness (I_0) to produce the polarization. The difference in the double loop orientations between the scattering and the MI models (see Figs. 7 and 8) is due to the 90° angular shift in the scattering model (linear polarization is perpendicular to the scattering plane; eqs. [9] and [10]) plus the Faraday rotation in the MI model (eqs. [1] and [2]). As a way to distinguish the source of polarization, the difference may be of minor significance, since the orientations of the rotation axes of single stars are rarely known. The phase dependence of the variations may, however, turn out more useful in distinguishing the source, as demonstrated by Figure 9, where the models of Figure 7 are plotted against phase for the case of scattering (*solid line*) and MI (*dashed line*). A detailed phase by phase study of the P variations from sufficiently accurate observations might thus provide adequate constraints as to the source of polarization.

The deviation from linear scaling in the scattering model differs slightly from that of the MI model which is demonstrated by Figure 10 (to be compared with Fig. 3). The maximum polarization is achieved with spot sizes of $f = 18\%$. We have made a polynomial fit, analogous to equation (3), to find the approximate spot size dependence of the scattering-induced linear polarization. The resulting formula

$$\frac{P_{\max}(f)}{P_{\max}(f = 1\%)} = 1.192 \times 10^{-2} + 1.048f - 6.945 \times 10^{-2}f^2 + 2.246 \times 10^{-3}f^3 - 3.592 \times 10^{-5}f^4 + 2.255 \times 10^{-7}f^5 , \quad (13)$$

where f is expressed in percent, applies at least for $f \leq 50\%$, and the scaling is linear with the scattering optical depth τ_s (as long as the optically thin approximation holds). The symmetry relation mentioned in conjunction with equation (3) also holds for equation (13), and therefore in the most favorable case (two polarizing regions at opposite directions from the stellar disk center), the polarization could be twice the value given by equation (13).

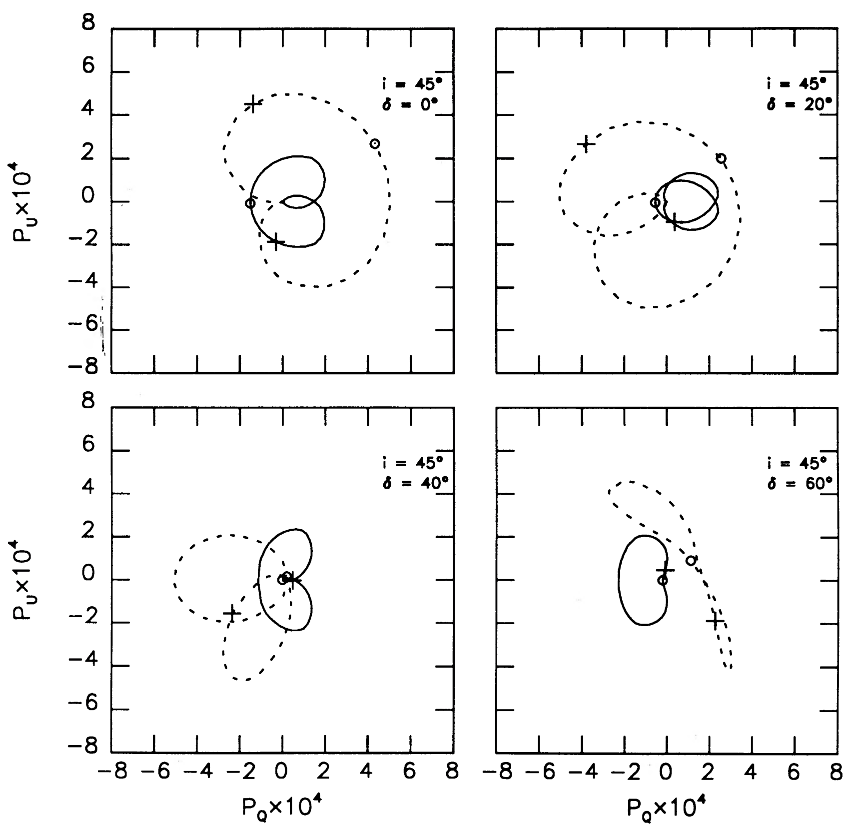

FIG. 7.—Scattering models (*solid lines*) for one $f = 5\%$ spot with different stellar inclinations, assuming $\tau_s = 0.1$ and equal brightness inside and outside of the spot.

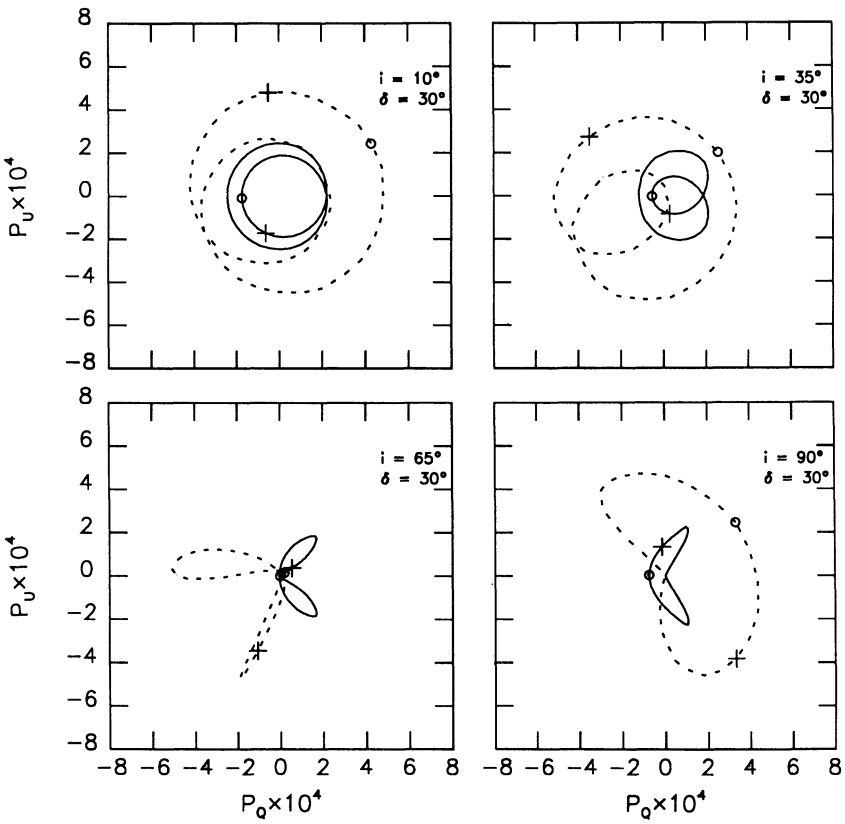

FIG. 8.—As in Fig. 7, but for spots with different latitudes

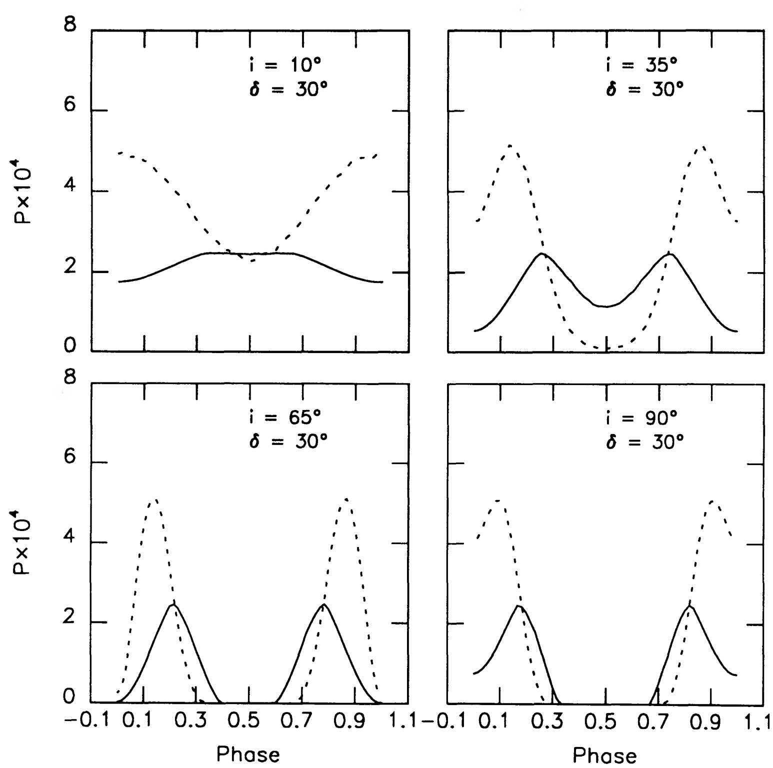

FIG. 9.—Comparison of P vs. rotational phase for the models of Fig. 7. The scattering model is shown by the continuous line and the MI model by the dashed line.

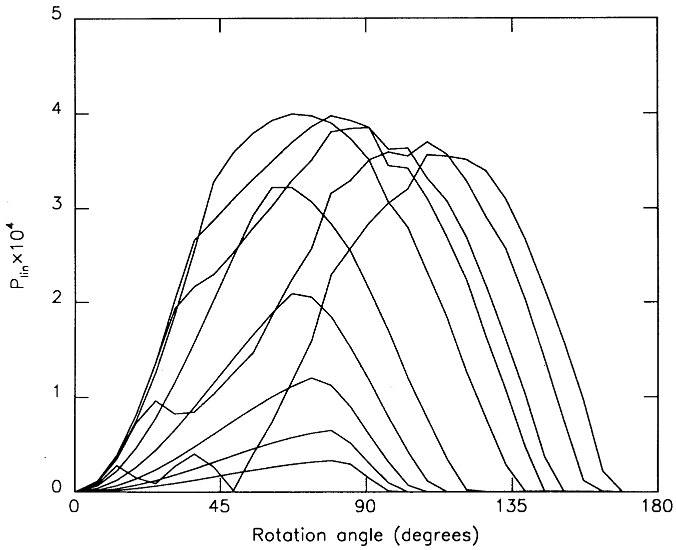

FIG. 10.—P vs. line-of-sight angle (i.e., rotation angle) for the scattering models (compare with Fig. 3 which shows the corresponding MI models). The curves are for spot sizes of $f = 0.5$, 1, 2, 4, 8, 18, 25, 30, 40, and 50%. The largest polarization is achieved with an $f = 18\%$ spot. The small secondary maxima for spots with $f = 40\%$ and 50% are due to geometrical effects and cancellation which become important in large regions.

The frequently used $\sin^2 \psi$ dependence for Rayleigh scattering, although valid for a single point at the surface, also does not directly apply for the total polarization in finite-size magnetic regions. The line-of-sight angle of the maximum polarization differs from 90° by an amount that depends on the spot size (see Fig. 10). It is close to 90° for very small spots ($f \ll 1\%$), decreasing to about 60° for $f = 10\%$ spots, and with areas larger than this the maximum shifts back toward (and finally beyond) the limb. The above effects are consequences of partial cancellation and geometrical effects which become important with large polarizing areas, analogous to, although not identical with, the MI case.

As for the scales of the models in Figures 7 and 8, we note that we have chosen an optimum value of the scattering optical depth ($\tau_s = 0.1$). The predicted contribution of free electrons in the solar chromosphere, for instance, adds up to a considerably smaller optical depth. Considering a typical value for $\overline{n_e} \approx 10^{11}$ cm^{-3} in the solar chromosphere and a thickness of 10^4 km (rough overestimate for the solar chromosphere), we obtain $\tau_s \approx 10^{-4}$. The resulting disk-integrated polarization due to Thomson scattering, using the total filling factor of active areas ($f = 1\%$–2%), will be less than $10^{-5}\%$ (i.e., 10^{-7} in absolute units), which is well below the threshold of detection. For typical atomic and molecular polarizabilities (e.g., Allen 1955), BLP due to Rayleigh scattering will be larger than for Thomson scattering. Thus, stars with outer atmospheres much deeper and/or denser than in the Sun may show enhanced contributions to BLP from scattering.

We also emphasize that, in addition to considerable optical thickness, inhomogeneous structure in the scattering atmosphere is necessary to produce nonzero disk-integrated polarization (just as in the MI case). More precise estimates of τ_s, and hence the relative contribution of scattering to BLP, can be made by using chromospheric models. These will be investigated in a companion paper (Paper II).

4. DISCUSSION AND CONCLUSIONS

We have developed improved models of magnetically induced broad-band linear polarization which include explicit disk integration of Stokes Q and U parameters over the stellar surface. The results show that scaling polarization linearly with spot size (L82) generally overestimates the rotational variations of polarization. The differences are negligible with regions smaller than 1% of a stellar hemisphere but increase rapidly with the region size, and are more than one-fifth of the maximum polarization with an $f = 5\%$ region (see Figs. 1 and 2). The overestimates are due to the neglect of the self-cancellation of the Stokes parameters *within* finite-sized magnetic regions. The superiority of explicit disk-integration also becomes evident with regions near, or partly behind, the stellar limb.

The calculations with disk integration show that the polarization increases nonlinearly with spot size, reaching an upper limit for a region with $f \approx 24\%$. Further increase in the circular region size produces a decrease in the polarization, again due to the self-cancellation effects (Figs. 3 and 4). The line-of-sight angle of the maximum polarization also depends on the spot size, generally deviating from the value 45° given by the linear scaling approximation (L82). The maximum polarization curve in Figure 4 can be used to set upper limits to the BLP expected in cool stars, and in estimating lower limits for the magnetic area filling factors from the observed linear polarization (Paper II). For this purpose, we have derived an approximate formula (eq. [3]) by fitting a fourth-order polynomial to the curve of the disk-integrated polarization in Figure 4.

We find that the effects of bipolar structure in the magnetic field are strongly dependent on the scale of the bipolar regions (Figs 5 and 6). Regions composed of small-scale bipolar elements exhibit complete cancellation of Faraday rotation. Rotational variations are close to those in the corresponding unipolar regions. The variations become significantly different if the small-scale bipolarity is replaced by large-scale bipolarity (i.e., a large bipolar spot pair). The former situation is analogous to the solar case, having groups of small bipolar spot pairs. The observations of the circular polarization in late-type (G–M) stars also support this scenario, since large values have not been found (e.g., Borra et al. 1984).

Rayleigh and Thomson scattering may also produce significant linear polarization in late-type stars. We have therefore developed analogous disk-integrated models for polarization due to scattering. Like the MI case, scattering-induced BLP shows an upper limit (at $f \approx 18\%$) due to cancellation effects. We introduce an approximate formula (eq. [13]) for the scaling of scattering the induced polarization as a function of the region size, which can be used for filling factor determinations, analogous to equation (3). The actual values obtained for the polarization are, however, probably too high, which is due to our assumption of optimal value (0.1) for τ_s. Values of τ_s and the resulting linear polarization in stars are estimated in Paper II.

Our models show that for scattering regions of finite size, the line-of-sight angle, at which the polarization due to Rayleigh scattering peaks, can deviate significantly from the normally expected 90° (again due to the spatial cancellation effects; see Fig. 10). This angle is generally different from the angle at which the MI induced polarization reaches a maximum (Fig. 3). The difference may be detectable (see Fig. 9), but this requires accurate observations in many rotational phases.

The values of the parameters used here, which determine the scale in the MI models, are generally reasonable for stars. The models are not complete, however, since the line-blanketing parameter ξ and the line-to-continuum opacity ratio η_0 may differ significantly from the arbitrarily chosen values (0.1 and 10, respectively). In fully self-consistent models, these parameters cannot be defined independently, since ξ is physically related with η_0. Accurate determination of broad-band values of these quantities is not a trivial task and requires knowledge of the mean line density and strength as a function of wavelength. Also, as pointed out by Leroy (1989), the contribution of molecular lines should be determined, since molecules increase the observed ξ, but appear to contribute little to the linear polarization. In a very recent investigation, Leroy (1990) found that significant blending of lines (crowded spectra) causes further decrease in the linear polarization (parameter C in eqs. [1] and [2]). We consider a simple model for estimating the wavelength dependence of MI polarization and discuss the above effects in a companion paper (Paper II; see also Saar and Huovelin 1990b).

Finally, the application of our models to real data deserves some comment. Since the overall levels of BLP due to MI or scattering are in most cases close to the detection limits, it is important to be extremely careful in determining the instrumental and possible interstellar (or any other constant) components of polarization if the polarization degree P is to be used for comparisons with models. An unknown, additional polarization component may significantly alter the rotational variations of P (e.g., Fig. 9) and will disqualify direct comparisons with our models. The value of P, however, is unaffected by the orientation of the stellar rotation axis on the sky.

In contrast, use of P_Q and P_U (instead of P) when fitting data has the advantage that the models (e.g., Figs 5–8) are identical, except for a shift of the zero point, if any (constant) errors in the polarization exist. The orientation of the stellar rotation axis will, however, affect the relative changes of P_Q and P_U. If this orientation is not known, comparison with models is ambiguous to within an arbitrary rotation of the coordinate system. We may conclude from the above that P should be modeled if interstellar and instrumental polarization can be accurately determined, and the orientation is unknown, and P_Q and P_U should be modeled if the reverse is true. If either the external polarization or the orientation can be determined, the other parameter can, in principle, be derived from the observations by using an appropriate fitting procedure.

This research was supported by a grant from the Emil Aaltonen Foundation (J. H.), the Smithsonian Institution Postdoctoral Fellowship program (S. S.), NASA grant NAGW-112 (S. S.), and Interagency transfer W-15130 (S. S.). S. S. is grateful for the hospitality shown him at the University of Helsinki, where some of this work was completed. The work presented here was begun while both authors were at the Joint Institute for Laboratory Astrophysics, where S. S. was supported by NASA grant NGL-006-03-057 to the University of Colorado, and J. H. a grant for project 01/191 from the Academy of Finland. We thank an anonymous referee for helpful suggestions.

REFERENCES

Allen, C. W. 1955, Astrophysical Quantities (London: Athlone), p. 87
Aller, L. H. 1953, Astrophysics: The Atmospheres of the Sun and Stars (New York: Ronald), p. 125
Barbour, M. S., & Kemp, J. C. 1981, ApJ, 246, 203
Borra, E. F., Edwards, G., & Mayor, M. 1984, ApJ, 284, 211
Brown, J. C., & McLean, I. S. 1977, A&A, 57, 141
Brown, J. C., McLean, I. S., & Emslie, A. G. 1978, A&A, 68, 415
Calamai, G., & Landi Degl'Innocenti, E. 1983, A&AS, 53, 311 (CL)
Calamai, G., Landi Degl'Innocenti E., & Landi Degl'Innocenti, M. 1975, A&A, 45, 297
Cayrel, R., Cayrel de Strobel, G., Campbell, B., Mein, N., Mein, P., & Dumont, S. 1983, A&A, 123, 89
Collins, G. W., II 1988, MNRAS, 234, 417
Doherty, L. R. 1986, ApJ, 307, 261
Finn, G. D., & Jefferies, J. T. 1974, Solar Phys., 39, 91
Finn, G. D., & Kemp, J. C. 1974, MNRAS, 167, 375
Hayes, D. P. 1984, ApJS, 55, 179
Huovelin, J., Linnaluoto, S., Piirola, V., Tuominen, I., & Virtanen, H. 1985, A&A, 152, 357
Huovelin, J., Linnaluoto, S., Tuominen, I., & Virtanen, H. 1989, A&AS, 78, 129
Huovelin, J., Piirola, V., Vilhu, O., Efimov, Y. S., & Shakhovskoy, N. M. 1987, A&A, 176, 83
Huovelin, J., & Saar, S. H. 1990, in Cool Stars, Stellar Systems, and the Sun, ed. G. Wallerstein, (ASP Conf. Ser., 9), p. 174
Huovelin, J., Saar, S. H., & Tuominen, I. 1988, ApJ, 329, 882
Kemp, J. C., & Wolstencroft, R. D. 1974, MNRAS, 166, 1
Landi Degl'Innocenti, E. 1982, A&A, 110, 25 (L82)
Landi Degl'Innocenti, E., & Calamai, G. 1982, A&AS, 49, 677
Landi Degl'Innocenti, M., Calamai, G., Landi Degl'Innocenti, E., & Patriarchi, P. 1981, ApJ, 249, 228
Landolfi, E., Landi Degl'Innocenti, M., & Landi Degl'Innocenti, E. 1989, A&A, 216, 113
Leroy, J. L. 1962, Ann. d'Ap, 25, 127
———. 1989, A&A, 215, 360
———. 1990, A&A, 237, 237
McCall, A., & Hough, J. H. 1980, A&AS, 42, 141
Mullan, D. J., & Bell, R. A. 1976, ApJ, 204, 818
Piirola, V. 1977, A&AS, 30, 213
———. 1980, A&A, 90, 48
Poe, C. H., & Eaton, J. A. 1985, ApJ, 289, 644
Rodonò, M., et al. 1986, A&A, 165, 135
Saar, S. H., & Huovelin, J. 1990a, ApJ, submitted (Paper II)
———. 1990b, in Cool Stars, Stellar Systems, and the Sun, ed. G. Wallerstein (ASP Conf. Ser., 9), p. 85
Schwarz, H. E., & Clarke, D. 1984, A&A, 132, 370
Serkowski, K. 1970, ApJ, 160, 1083
Shakhovskoi, N. M. 1965, Soviet Astr.–AJ., 8, 833
Shulov, O. S. 1967, Astrofizika 3, 233
Tinbergen, J. 1982, A&A, 105, 53
Tinbergen, J., & Zwaan, C. 1981, A&A, 101, 223
van de Hulst, H. C. 1957, Light Scattering by Small Particles (New York: Wiley and Sons)